Rheological behaviour and spectroscopic investigations of cerium-modified AlO(OH) colloidal suspensions

Rudina Bleta *, Olivier Jaubert, Marie Gressier, Marie-Joëlle Menu

Université de Toulouse, Institut Carnot CIRIMAT UMR 5085 UPS/INPT/CNRS, Université Paul Sabatier, 118 route de Narbonne, 31062 Toulouse Cedex 9, France

Keywords:
Colloid
Boehmite
Thixotropy
Cerium
Vibrational spectroscopies

A B S T R A C T

The rheological behaviour of aqueous suspensions of boehmite (AlO(OH)) modified with different Ce-salts ($Ce(NO_3)_3$, $CeCl_3$, $Ce(CH_3COO)_3$ and $Ce_2(SO_4)_3$) was investigated at a fixed Ce/Al molar ratio (0.05). Freshly prepared boehmite suspensions were near-Newtonian and time-independent. A shear-sensitive thixotropic network developed when Ce-salts with monovalent anions were introduced in the nanoparticle sols. The extent of particle aggregation dramatically increased with ageing for $Ce(NO_3)_3$ and $CeCl_3$ whereas an equilibrium value was reached with $Ce(CH_3COO)_3$. The addition of $Ce_2(SO_4)_3$ with divalent anions involved no thixotropy but rather a sudden phase separation.

The combined data set of IRTF and DRIFT spectra indicated that free NO_3^- anions of peptized boehmite adsorb on the nanoparticle surface by H-bond. The introduction of Ce-salts in the boehmite sol led to the coordination between Ce^{3+} ions and NO_3^- anions adsorbed on boehmite *i.e.* to $[Ce(NO_3)_4(H_2O)_x]^-$ complex. Such coordination led to a thixotropic behaviour which was lower with $Ce(NO_3)_3$ compared to $CeCl_3$ and $Ce(CH_3COO)_3$. In contrast, $Ce_2(SO_4)_3$ formed insoluble complexes with dissolved aluminium species. The formation of H-bonded surface nitrate complexes was found to play a decisive role on the particle–particle interactions and consequently on the rheological behaviour of the sols.

1. Introduction

Colloids with anisotropic shape and nanometre dimensions present a host of unusual properties that set them apart from spherical isotropic suspensions. When dispersed in aqueous media, these systems exhibit high stability against precipitation or phase separation and interesting phenomena such as streaming birefringence and thixotropy [1]. These properties, which originate from the particle orientation and spatial organisation, have been the subject of intense investigations from both theoretical [2] and experimental [3] points of view. When concentrated, these sols become progressively less fluid and the rheological response of the liquid changes from near-Newtonian (strong repulsive inter-particle forces) to thixotropic (formation of an inter-particle network) [4,5]. Under flow conditions, this network slowly breaks-down into smaller aggregates and it builds-up on standing. The existence of such network reconstruction mechanism is the main difference between a thixotropic sol and a gel.

Thixotropic effects are exhibited by a large array of colloidal systems such as paints, clay suspensions, emulsions, bitumes, biological fluids [6]. For a large-scale production of surface coatings, a thixotropic sol is highly desirable because its gelling occurs rapidly enough to prevent the sol running down the vertical surfaces during drying process [7,8]. This minimises the caking troubles *i.e.* formation of a compact hard mass at the bottom of the substrate when the sol settles down.

Among different colloidal anisotropic suspensions, boehmite crystallites have received widespread attention due to their use in numerous applications such as catalysis [9], cosmetics [10] and paints [11]. Boehmite crystalline structure is planar and built-up of oriented sheets of octahedral aluminium units connected *via* hydrogen bonds [12]. Boehmite sols may be prepared by different ways: by decomposition of aluminium hydroxide ($Al(OH)_3$) under controlled conditions of temperature and pressure [13], by precipitation in acid [14] or basic media [15] or by sol–gel route [16a–d]. The advantages of preparing boehmite by sol–gel route from metal alkoxides include the high purity of the starting material, the opportunity to mix different cations at the molecular level to yield a homogenously doped product, the small size of the particles in the colloidal sol and the lack of contaminating ionic byproducts [17].

Rheological studies on isotropic colloidal suspensions of titania have been performed in our group [18] and the spatial organisation

* Corresponding author. Present address: Equipe Physico-chimie des Colloïdes, UMR SRSMC no. 7565, Université Henri Poincaré, Nancy 1/CNRS Faculté des Sciences, BP 239, F-54506 Vandoeuvre-lès-Nancy Cedex, France. Fax: +33 3 83 91 25 32.

E-mail addresses: rudina.bleta@srsmc.uhp-nancy.fr (R. Bleta), jaubert@chimie.ups-tlse.fr (O. Jaubert), gressier@chimie.upstlse.fr (M. Gressier), menu@chimie.ups-tlse.fr (M.-J. Menu).

doi:10.1016/j.jcis.2011.08.008

of particles has been related to the porosity of the final material [19]. On the other hand, anisotropic boehmite suspensions have been investigated in a number of experiments under various conditions of electrolyte content, pH range [20] and peptizing acid [21]. These experiments show that monovalent anions interact electrostatically with the superficial charge of particles. As a result of these interactions, the diffuse part of the double layer is compressed and the repulsions between the particles are reduced. This leads to particle aggregation and to gel formation when a critical ionic strength is reached [17]. The addition of divalent anions such as SO_4^{2-}, [17,22–24] was found to involve a strong coagulating effect which is attributed to a higher complexing ability of this anion with dissolved aluminium species and to the formation of insoluble complexes such as $Al_2(SO_4)(OH)_4$ [23] or $Na[Al_{13}O_4(OH)_{24}(H_2O)_{12}(SO_4)_4]$ [22,25]. The presence of such complexes on the surrounding water also contributes to the progressive reduction of the diffuse portion of the double layer leading to agglomeration and/or precipitation.

One particularly interesting area in terms of applications is the use of boehmite as support for the immobilization of rare-earth metal ions because of its high surface area (~450 $m^2\,g^{-1}$) [26] coupled with favourable surface properties (hydroxyl groups). Among rare-earth metal ions, cerium is of particular interest in different areas including catalysis [27], corrosion protection [28,29], and diesel fuel applications [30]. In catalysis, cerium has been used as a promoter in the selective catalytic reduction (SCR) of NO_x by methane improving oxidation of NO while protecting CH_4 from combustion [27]. Furthermore, the incorporation of Ce^{3+} ions in mesoporous alumina has been shown to dramatically improve the thermal stability of the catalyst by reducing sintering [31]. In corrosion protection of aluminium alloys, it has been reported that some of the most effective and environmentally friendly corrosion inhibitors are derived from Ce-salts [28,29]. Ce-doped zirconia nanoparticles incorporated in a sol–gel matrix of an organoalkoxysilane have been demonstrated to act as nanoreservoirs providing a prolonged release of the inhibitor [32]. Such a phenomenon is believed to result from the deposition of hydrated cerium oxide on the cathodic intermetallic particles existing in the aluminium alloy, contributing thereby to the suppression of the cathodic reaction [33].

These experiments confirm that cerium ions interact strongly with oxide nanoparticles. However, most of these investigations identify neither the molecular structure of nanoparticle surface complexes nor the bonding mode of cerium salts at the mineral–water interface. Considerably less attention has been paid to the effect of cerium on the rheological behaviour of colloidal suspensions of boehmite, despite the importance of this parameter in the quality of the coats. In the present study, the spectroscopic data (DRIFT, ATR and Raman) indicate that $[Ce(NO_3)_4(H_2O)_x]^-$ complex ions that form at the boehmite surface play a decisive role in the rheological behaviour of the colloidal suspensions. Our results demonstrate that, according to the type of Ce-salt used, one may considerably extend the rate of thixotropic structure and the sol viscosity. To our knowledge, there is no spectroscopic study in the literature which explains the interplay between the bonding mechanism of lanthanides on the nanoparticle surface and the rheological behaviour of the sols.

2. Experimental section

2.1. Synthesis of boehmite colloids

Boehmite nanoparticles were synthesised by a sol–gel method reported by Yoldas [16a–d]. The final product was a transparent suspension of boehmite nanoparticles at pH 4.3. The concentration of aluminium in the sol was 0.5 mol L^{-1} as determined by weight loss on ignition at 1000 °C for 2 h [26]. Subsequently, aliquots of boehmite suspensions were introduced into 40 mL tubes and different amounts of $Ce(NO_3)_3{\cdot}6H_2O$ (Acros), $CeCl_3{\cdot}7H_2O$ (Acros), $Ce(CH_3COO)_3{\cdot}xH_2O$ (Aldrich) and $Ce_2(SO_4)_3{\cdot}xH_2O$ (Aldrich) were introduced according to a Ce/Al molar ratio fixed for all experiments at 0.05. The mixtures were stirred for 6 h at room temperature until complete dissolution of the salts. The samples were then stored at room temperature for 3 days. Xerogels were obtained after drying 20 mL sols by evaporation at 40 °C for 48 h in an oven. Powders were grounded before characterisation.

2.2. Characterisation methods

Rheological analyses were performed on freshly-prepared and 3 days-aged samples with a rheometer Anton Paar Physica MCR fitted with a cone and plate device. The dimensions corresponding to the geometry were 50 mm for the diameter and 1° for the angle. The minimum distance between plate and truncated cone was 0.05 mm. Rheograms were recorded at 20 °C with shear-rate being stepwise increased and decreased over the range of 1–1000 s^{-1} over a total time period of 300 s for both the increasing and decreasing shear-rate sweeps. The thixotropic structure that develops in Ce-modified boehmite suspensions was evaluated by measuring the area enclosed between the up- and down- curves in the shear-stress *vs.* shear-rate data. Herschel Bulkley's rheological model was adopted to fit the downward flow curve of the hysteresis loop and to estimate the rheological parameters of freshly-prepared (t_0) and 3 days-aged (t_{3d}) sols. Zeta potential measurements were collected with a Zetasizer nano ZS 90 Malvern equipped disposable capillary cells. All measurements were done at 25 °C, with a scattering angle of 90°. Powder X-ray diffraction (PXRD) data were collected on a Bruker D4 Endeavor X-ray diffractometer in a Bragg Brentano configuration with Cu Kα radiation source at 40 kV and 40 mA. Scans were run over the angular domain $10° < 2\theta < 80°$ with a step size of 0.016°. Crystalline boehmite was identified by comparing the experimental diffraction patterns to Joint Committee on Powder Diffraction Standards (JCPDS) powder diffraction file. Transmission electron microscopy (TEM) observations were performed with a JEOL-JEM-1400 microscope operating at 120 kV at medium magnification. Fourier transformed infrared spectra were collected in the 4000–400 cm^{-1} range with a resolution 4 cm^{-1} on the Bucker Vector 22 spectrophotometer coupled with OPUS software. Powders were compacted in KBr lattice (1% by weight). Diffuse Reflectance Infrared Fourier Transform (DRIFT) analyses were performed in a Perkin–Elmer 1760 X spectrometer equipped with Deuterated Triglycine Sulphate (DTGS) detector. The ATR–FTIR spectra were recorded using a Nicolet 510P Nexus spectrophotometer equipped with DTGS detector. Boehmite was deposited on a Germanium crystal. The deposited suspension was allowed to dry under N_2 atmosphere.

3. Results

3.1. Characterisation of boehmite crystallites

Fig. 1 shows a typical TEM micrograph of boehmite nanoparticles which appear as anhedral laths. A closer look at these laths reveals that they are built-up of smaller plate-like particles which show a local packing. A mesoporous structure is formed through the aggregation of these laths. XRD diffraction pattern (inset) reveals that particles are comprised of crystalline boehmite (JCPDS card no 21-1307) whose structure corresponds to an orthorhombic unit cell (space group number 63, *Amam*) [34].

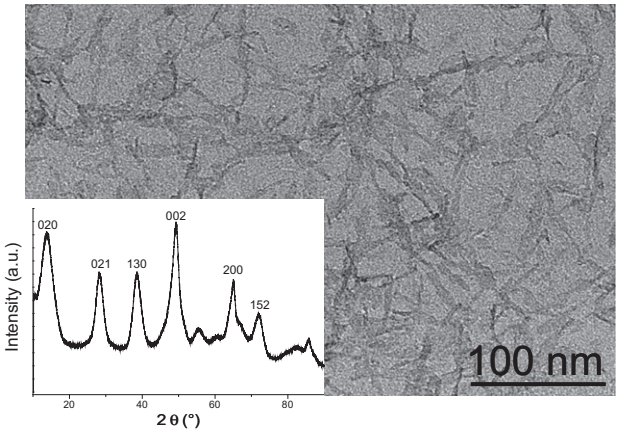

Fig. 1. TEM micrograph and XRD pattern (inset) of boehmite crystallites (JCPDS card no. 21-1307).

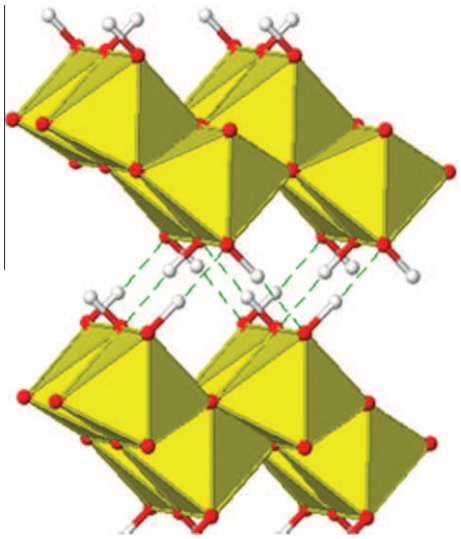

Fig. 2. Drawing of γ-AlO(OH) boehmite structure.

The unit cell of boehmite (Fig. 2) consists of two double layers of $AlO_4(OH)_2$ aluminium-centred distorted octahedra. Hydroxyl groups are located at the outer surface of the double layers and they interact to hold the layers together.

Fig. 3 shows a representative FTIR spectrum of air-dried boehmite xerogels recorded in the 4000–400 cm^{-1} region. The vibration modes of boehmite are assigned in agreement with Fripiat [35] and Colomban [36]. In addition to the vibration modes of boehmite shown on the figure, the broad bands at 3409 and 1630 cm^{-1} are assigned to the stretching and bending vibration modes of adsorbed water. The peak at 1380 cm^{-1} corresponds to free NO_3^- anions from HNO_3 added for peptization [37]. This peak was not observed in the boehmite peptized with HCl (spectrum not shown).

3.2. Flow behaviour of boehmite suspensions modified with $Ce(CH_3COO)_3$

Boehmite suspensions modified or not with $Ce(CH_3COO)_3$ were submitted to rheological measurements in order to investigate the extent of particle aggregation. Fig. 4 shows shear-stress *vs.* shear-rate (a) and apparent viscosity *vs.* shear-rate (b) curves for boehmite and $Ce(CH_3COO)_3$-modified boehmite. Freshly prepared Ce-free boehmite presents a near-Newtonian behaviour since shear-stress *vs.* shear-rate curve is near linear passing through the origin. This sol displays a constant value of viscosity (1.5 mPa s) over the entire range of shear-rates (0–1000 s^{-1}). On the other hand, the addition of $Ce(CH_3COO)_3$ induces a shear-thinning thixotropic behaviour, *i.e.* the viscosity decreases with increasing shear-rate and the flow-curve presents an hysteresis loop. Such a thixotropic behaviour is typical of disc-shape nanoparticles [38]. It describes a reversible transition from a flowable fluid to a solid-like elastic gel [39]. Under flow conditions, the structure of this gel slowly breaks-down into smaller aggregates and the viscosity decreases over time. On standing, the network builds-up and viscosity increases.

The formation of such a gel results from the attractive interactions between particles. According to Derjaguin, Landau, Verwey, and Overbeek (DLVO) theory [40], when van der Waals attractive forces dominate, the particles form either reversible aggregates (controlled by physical forces) or irreversible agglomerates (arising from chemical reactions) [41]. We will see in what follows that depending on the type of counterion used, these two types of interactions can occur in boehmite sols.

3.3. The influence of type of cerium salt

In this section we consider different Ce-salts ($Ce(NO_3)_3$, $CeCl_3$, $Ce(CH_3COO)_3$ and $Ce_2(SO_4)_3$) to highlight the effect of the counterion on the boehmite particle aggregation and on the network formation. In all experiments, the Ce/Al molar ratio was fixed at 0.05.

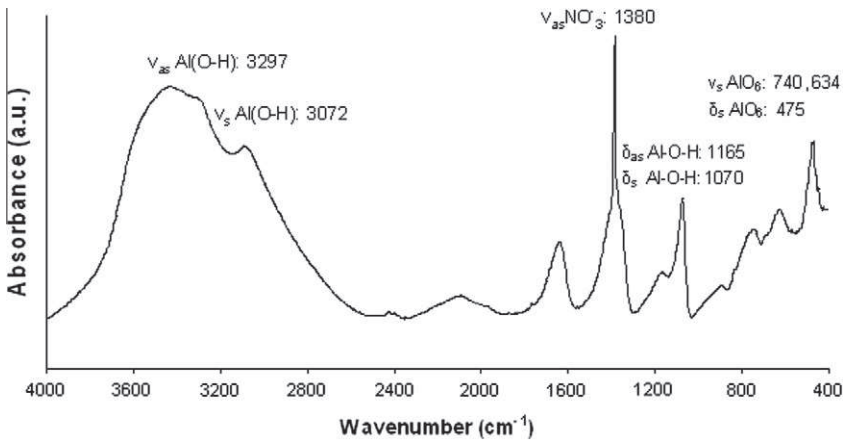

Fig. 3. FTIR spectra of boehmite xerogel.

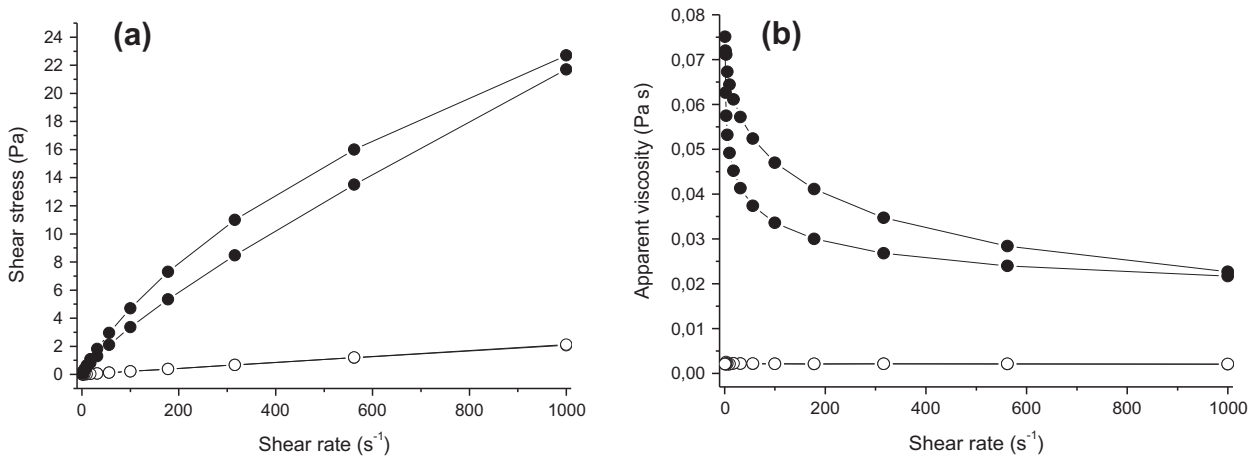

Fig. 4. Shear-stress *vs.* shear-rate (a) and viscosity *vs.* shear-rate curves (b) for Ce-free (○) and $Ce(CH_3COO)_3$-modified boehmite (●).

Fig. 5 shows the shear-stress *vs.* shear-rate curves for freshly prepared (a) and aged (b) boehmite sols modified with the four Ce-salts. As described previously, boehmite suspensions are initially (at t_0) highly stabilized by repulsive forces between the particles and present a near-Newtonian behaviour.

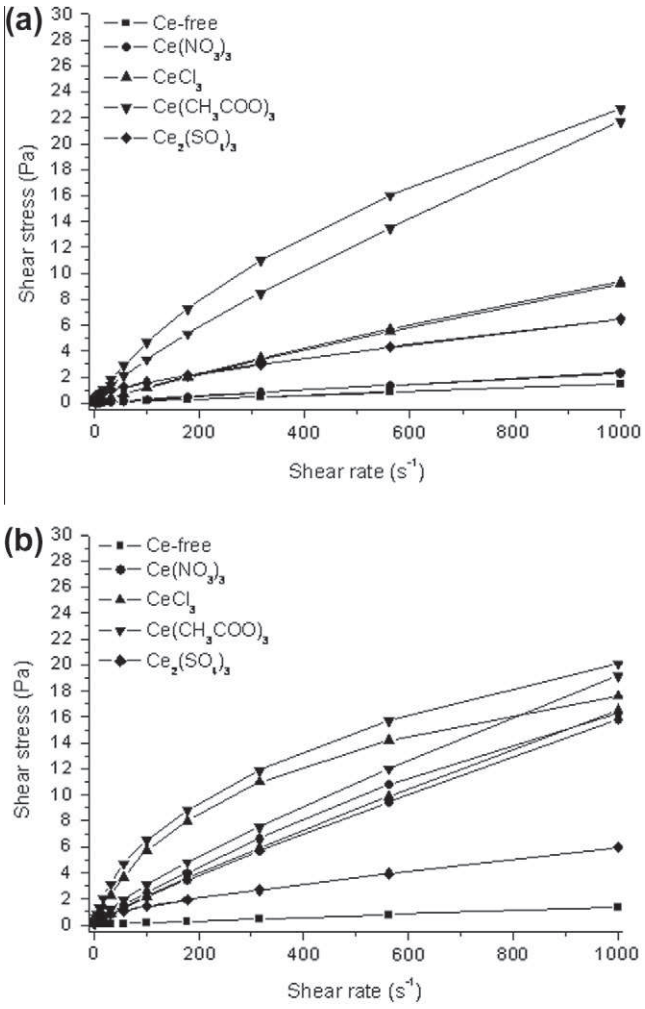

Fig. 5. Shear-stress *vs.* shear-rate curves for freshly prepared (a) and 3 days-aged (b) suspensions of boehmite modified with different cerium salts.

Upon addition of $Ce(NO_3)_3$ and $CeCl_3$, a slight hysteresis loop is observed indicating the beginning of the structure formation. On the other hand, $Ce(CH_3COO)_3$ develops a strong shear-thinning thixotropic behaviour immediately after being introduced in the nanoparticle sol. The flow curve of this sol is characterised by a large hysteresis loop, indicating strong adhesive interactions between particles.

Apparent viscosities measured at $1000\ s^{-1}$ follow the same trend as the thixotropy, increasing in the order: $Ce(NO_3)_3$ (2.21 mPa s) < $Ce_2(SO_4)_3$ (6.48 mPa s) < $CeCl_3$ (9.33 mPa s) < $Ce(CH_3COO)_3$ (23.29 mPa s) (Table 1). When the suspensions were aged for 3 days, the apparent viscosity of non-modified boehmite was not changed and its flow-behaviour was time-independent (Fig. 5b). On the other hand, the flow curves of Ce-modified samples, except $Ce_2(SO_4)_3$, denoted a strong thixotropic behaviour. All those sols presented an increased shear-thinning behaviour which was more pronounced with $Ce(CH_3COO)_3$ and $CeCl_3$ compared to $Ce(NO_3)_3$. In contrast, $Ce_2(SO_4)_3$ showed no hysteresis loop and the viscosity further decreased to 5.94 mPa s after keeping the sol at rest for 3 days.

It is well-known that sulphates have stronger interactions with boehmite compared to nitrates and chlorides [23]. Such coordination generally leads to a chemical agglomeration that follows the particle aggregation [5]. Agglomeration is most likely to occur in our $Ce_2(SO_4)_3$-modified boehmite system. Indeed, all sols prepared with $Ce_2(SO_4)_3$ were white in colour and settled down at rest whereas those prepared with the other salts were transparent and stable.

The hysteresis area in the shear-stress *vs.* shear-rate data is expressed in $J\ m^{-3}\ s^{-1}$ and represents the physical energy per unit volume applied to the suspension per unit time to breakdown and build-up the internal structure [5,42,43]. Fig. 6 provides a comparison of the thixotropic structure that forms in boehmite sols modified with different Ce-salts at t_0 and t_{3d}. At t_0, $Ce(NO_3)_3$- and $CeCl_3$-modified boehmite show a low degree of thixotropy similar to boehmite. The addition of $Ce(CH_3COO)_3$ involved a strong

Table 1
Apparent viscosities measured at $1000\ s^{-1}$ in Ce-free and Ce-modified boehmite suspensions at t_0 and t_{3d}.

Boehmite sample	η_{t0} (mPa s)	η_{t3d} (mPa s)
Ce-free	1.52 ± 0.03	1.53 ± 0.03
$Ce(NO_3)_3$	2.21 ± 0.04	16.09 ± 0.32
$CeCl_3$	9.33 ± 0.19	17.23 ± 0.34
$Ce(CH_3COO)_3$	23.29 ± 0.47	19.72 ± 0.39
$Ce_2(SO_4)_3$	6.48 ± 0.13	5.94 ± 0.12

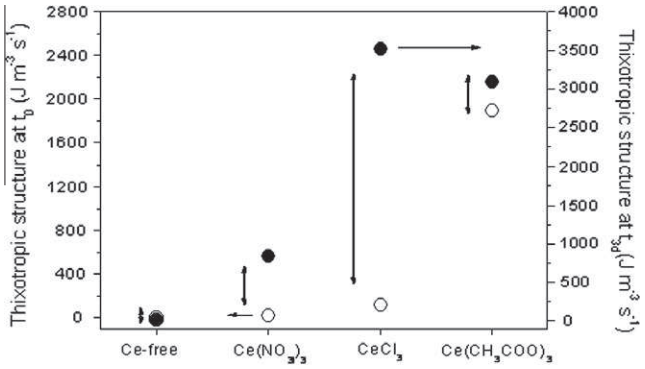

Fig. 6. Thixotropic structure formation at t_0 (○) and t_{3d} (●) represented by the area of hysteresis loop in shear stress *vs.* shear rate curve in the five colloidal boehmite suspensions.

increase of the thixotropic structure from 3.5 (Ce-free) to 1900 J m^{-3} s^{-1} (with $Ce(CH_3COO)_3$). Upon ageing for 3 days, Ce-free boehmite showed a time-independent behaviour since no thixotropic structure developed in this sol. Interestingly, the comparison between $Ce(NO_3)_3$ and $CeCl_3$ indicates that the thixotropic structure increases a little with the first salt (from 20 to 850 J m^{-3} s^{-1}) whereas this evolution is significant with the latter one (from 120 to 3500 J m^{-3} s^{-1}). On the other hand, a high thixotropic structure (1900 J m^{-3} s^{-1}) is reached suddenly with $Ce(CH_3COO)_3$ from the early introduction of this salt in boehmite sol and it increases up to 3100 J m^{-3} s^{-1} at t_{3d}.

Studies in literature show that very high values of thixotropy (about 2000 and 6000 J m^{-3} s^{-1}) can be attained with 20% *w/w* gibbsite (Al (OH)$_3$) particles when potassium and sodium cations are introduced respectively in the sol. Such rheological behaviour was attributed to the strong interactions between those cations and negatively charged particles [5].

We then applied Herschel Bulkley's rheological model [44] to estimate the rheological parameters at t_0 and t_{3d}. This model is written as:

$$\sigma = \sigma_0 + K\dot{\gamma}^n$$

where σ is the shear-stress, K is the consistency coefficient, $\dot{\gamma}$ is the applied shear-rate, σ_0 is the yield-stress when $\dot{\gamma}$ approaches zero and beyond which material begins to flow, n is the flow behaviour index. The results obtained by this model showed the best fitting performance ($\langle R^2 \rangle$ = 0.9999) when compared to the model of Bingham [45]. For $Ce_2(SO_4)_3$ modified boehmite, the Herschel Bulkley's model was not well-adapted to describe the rheological behaviour of this sol (fitting coefficient $\langle R^2 \rangle \sim 0.988$). The results on the modelling of this system are therefore not presented in the following.

Table 2 shows the values of the parameters computed from the analysed suspensions. In Ce-free boehmite and in boehmite modified with the three Ce-salts, the yield stress (σ_0) is negligible (<2 mPa at t_0 and <36 mPa at t_{3d}). This is consistent with the fact that the shear-thinning behaviour in these systems becomes visible from the early beginning of the applied yield-stress.

More evident differences between $Ce(NO_3)_3$, $CeCl_3$ and $Ce(CH_3COO)_3$ can be observed from the value of the coefficient of consistency K. At t_0, K significantly increases with $Ce(CH_3COO)_3$ as compared to $Ce(NO_3)_3$ and $CeCl_3$, whereas at t_{3d}, $Ce(NO_3)_3$ and $CeCl_3$ present the most rapid evolution. For $Ce(CH_3COO)_3$ and $Ce_2(SO_4)_3$, K decreases with ageing, following the same trend as the apparent viscosity (Table 1). On the other hand, n decreases after addition of Ce-salts, indicating that sols become less fluid.

In literature, K has not been reported for boehmite suspensions. The only data we have found concern dispersions of laponite [4a] which present a consistency coefficient about 2000 times higher (3.71 Pa s^n *vs.* 1.57 mPa s^n) compared to boehmite. This may be explained by the high capacity of laponite dispersions to form a viscoelastic gel due to the creation of house-of-cards structures [4a]. Such structures result from edge-to-face attractions between negative charges along the sides and positive charges along the edges of laponite [2a]. Indeed, the phase diagram of laponite [4a] indicates a sol–gel transition at about 2% *w/w* laponite while boehmite, at this concentration, is very fluid and non-thixotropic.

Table 2
Rheological parameters computed from Herschel Bulkley's rheological model in Ce-free and Ce-modified boehmite suspensions. σ_0 is the yield stress when the applied shear rate $\dot{\gamma}$ approaches zero, K is the coefficient of consistency and n is the flow behaviour index.

Boehmite sample	σ_0 (mPa)	K (mPa s^n)	n (–)	$\langle R^2 \rangle$ (–)
Ce-free-t_0	1.08 ± 0.55	1.57 ± 0.02	0.989 ± 0.002	0.99999
$Ce(NO_3)_3$-t_0	1.34 ± 0.65	3.73 ± 0.19	0.930 ± 0.007	0.99997
$CeCl_3$-t_0	1.44 ± 0.49	9.77 ± 0.37	0.882 ± 0.003	0.99998
$Ce(CH_3COO)_3$-t_0	2.35 ± 0.75	78.54 ± 1.23	0.814 ± 0.002	0.99999
Ce-free-t_{3d}	1.04 ± 0.75	1.70 ± 0.08	0.966 ± 0.007	0.99991
$Ce(NO_3)_3$-t_{3d}	3.18 ± 0.12	18.58 ± 0.68	0.882 ± 0.003	0.99998
$CeCl_3$-t_{3d}	20.61 ± 1.65	38.84 ± 1.04	0.867 ± 0.004	0.99996
$Ce(CH_3COO)_3$-t_{3d}	35.55 ± 2.11	73.37 ± 1.71	0.806 ± 0.003	0.99997

In order to evaluate the surface properties of Ce-modified boehmite suspensions, Zeta potential (ζ potential) measurements were then conducted in freshly prepared and 3 days-aged sols (Table 3). Zeta potential reflects the particle surface charge. It is known that the point of zero charge (PZC) of boehmite is near 9 [46,47]. For the sols synthesised at pH 4.3 (Ce-free boehmite), particles carry a positive charge (ζ = + 29 mV) which is attributed to the adsorption of H^+ ions on the Al-OH groups and to the formation of Al-$(OH_2)^+$ species. This charge is partially compensated by the counterions (NO_3^-) that are released in the aqueous phase during peptization. In the presence of Ce-salts, ζ potential decreases significantly (ζ = 0.5–3 mV) as the Ce-salts cover the surface of the particles and it takes negative values upon ageing. Moreover, depending on the nature of Ce-salt used, the pH of boehmite suspensions varies. At t_0, pH increases slightly from 4.3 (for Ce-free boehmite) to 4.4 (with $Ce(NO_3)_3$) and to 4.5 (with $CeCl_3$). This increase is more significant with $Ce_2(SO_4)_3$ (pH = 5.5) and with $Ce(CH_3COO)_3$ (pH = 5.5).

From these results, it appears that the addition of Ce-salts strongly affects the surface properties of boehmite and the rheological behaviour of the sol. In order to improve the understanding of surface chemistry controlling the processes occurring at boehmite–water interface, spectroscopic investigations were conducted in the following.

3.4. Spectroscopic investigations

DRIFT analyses were performed to obtain information about the bonding mode of Ce^{3+} ions at the boehmite–water interface. DRIFT spectroscopy provides an alternative to transmission infrared spec-

Table 3
ζ potential and pH of boehmite and Ce-modified boehmite measured at t_0 and t_{3d}.

Boehmite Sample	ζ potential at t_0 (mV)	ζ potential at t_{3d} (mV)	pH at t_0	pH at t_{3d}
Ce-free	29	29	4.3	4.3
$Ce(NO_3)_3$	0.5	−3.2	4.4	4.8
$CeCl_3$	1	−2.2	4.5	4.8
$Ce(CH_3COO)_3$	3	−2.8	5.5	5.6
$Ce_2(SO_4)_3$	1	−2.5	5.5	5.6

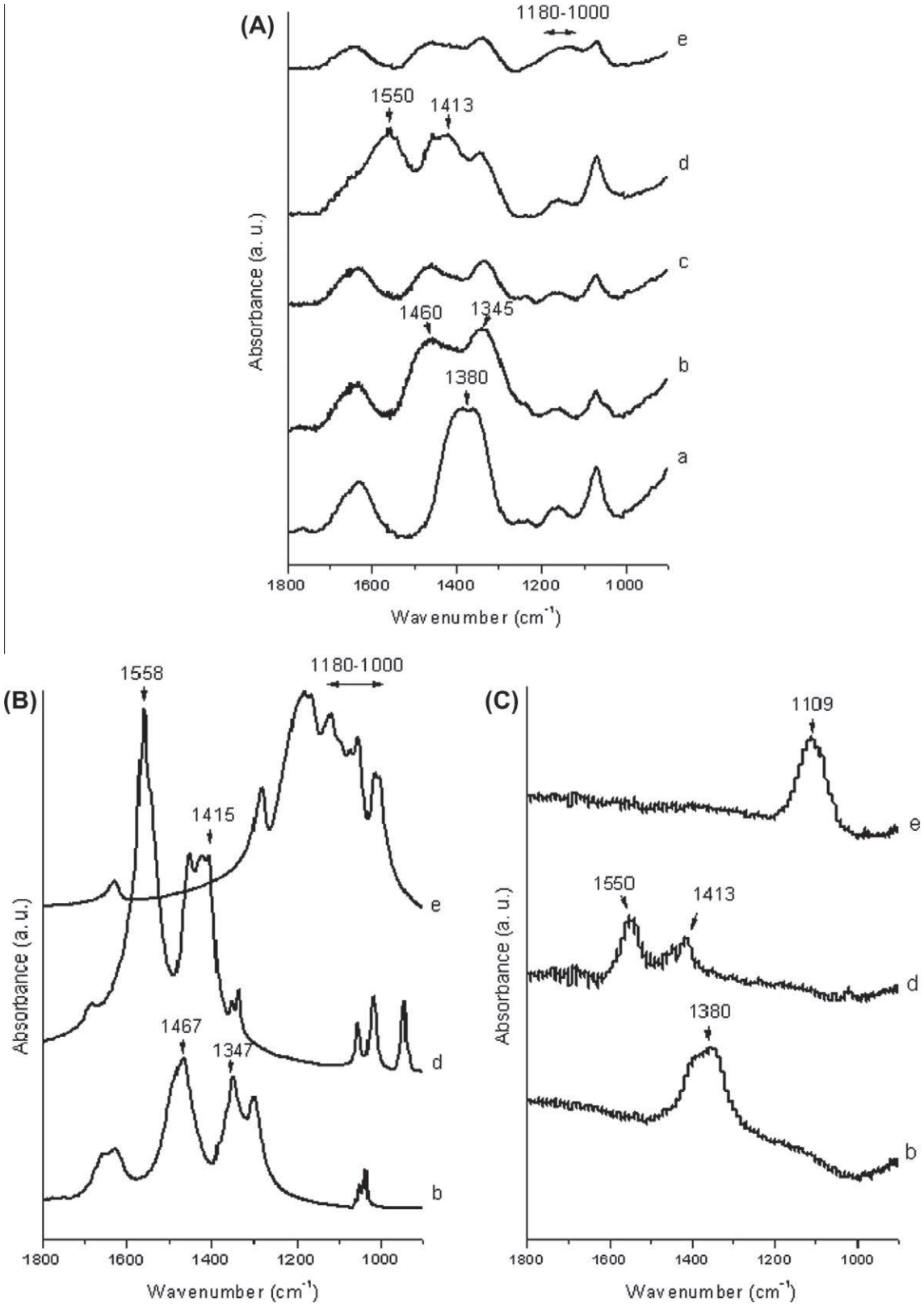

Fig. 7. DRIFT spectra (A) of boehmite (a) modified with different cerium salts: $Ce(NO_3)_3$ (b), $CeCl_3$ (c), $Ce(CH_3COO)_3$ (d) and $Ce_2(SO_4)_3$ (e). FTIR spectra of the four salts as solid (B) and ATR spectra in solution (C).

troscopy (FTIR) in that the integrity of the sample surface is ensured because no pressure is applied during sample preparation.

Fig. 7 A presents DRIFT spectra of Ce-free (a) and Ce-modified boehmite (b–e) in the range 1800–900 cm^{-1}. FTIR spectra of the four Ce-salts as solid (B) and ATR spectra of Ce-salts solubilised in aqueous media (C) are added for comparison (except chloride which is IR inactive). In Ce-free boehmite sample (A, a), the stretching vibration of free NO_3^- species from peptization appeared at

1380 cm^{-1}. This band is also observed in the spectrum of $Ce(NO_3)_3$ aqueous solution (C, b) which contains the hydrated cerium complex $[Ce(H_2O)_x]^{3+}$ and free nitrate anion. Upon addition of $Ce(NO_3)_3$ in the peptized boehmite sol (A, b), the band at 1380 cm^{-1} undergoes splitting into two bands, at 1460 and 1345 cm^{-1}, indicating a symmetry decrease of the anion. This can be compared with the presence of the two main characteristic vibrations of coordinated nitrate anions observed at 1467 and 1347 cm^{-1} in the spectrum of pure $Ce(NO_3)_3$ as a solid (B, b). Similarly to $Ce(NO_3)_3$, the spectra of $CeCl_3$–(A, c), $Ce(CH_3COO)_3$–(A, d) and $Ce_2(SO_4)_3$–(A, e) modified boehmite show the same splitting. So, we propose that a great portion of NO_3^- anions from peptization was coordinated with Ce^{3+} ions.

It is well-known that trivalent lanthanide ions, in their most stable state, give rise to high coordination number complexes and particularly in water where 8 to 11 chemical bonds are usually observed for simple complexes [48]. On the other hand, nitrate anion may exhibit two coordination modes (monodentate or bidentate) on a metal centre. Following this coordination different anionic complexes, such as $[Ce(NO_3)_4(H_2O)_x]^-$, which are in interaction with the boehmite nanoparticles, can form. Compared to nitrate and chloride, the sample containing acetate (A, d) present additional bands at 1550 and 1413 cm^{-1} which are also observed with this salt as solid (B, d) and in solution (C, d). In the case of $Ce_2(SO_4)_3$, the spectrum (A, e) is more flattened and the vibration bands of boehmite are less distinct and broader compared to the three other Ce-salts. However, even in this sample, it is evident that the peak at 1380 cm^{-1} assigned to NO_3^- anions undergoes splitting indicating that cerium exists in a coordinated state on the boehmite surface. The broadening of the spectra in the region from 1180 to 1000 cm^{-1} is probably due to the presence of numerous peaks from $Ce_2(SO_4)_3$ as solid in this region (B, e).

In attempt to obtain complementary information concerning the interactions between cerium and nitrate ions in solution, ATR–FTIR and Raman spectra were also collected in Ce-modified boehmite sols. Unfortunately the bands of water and butanol (which forms during hydrolysis of the aluminium tri-*sec*-butoxide) overlap the vibration bands of boehmite. The only information we have derived from Raman was a strong intensification of the band at 1050 cm^{-1} (vibration of NO_3^- anions) in the sample prepared with $Ce(NO_3)_3$. The other spectra did not provide accurate information to distinguish the behaviour of various salts.

4. Discussion

Due to their high reactivity towards water, aluminium alkoxides hydrolyse very rapidly in aqueous medium and nanoparticles form aggregates which precipitate. Peptization by means of an inorganic acid (HNO_3) is used to break down these large aggregates into small aggregates and primary particles of boehmite. The final result is a clear suspension which contains primary crystalline particles dispersed in water [16a].

The rheological data indicate that a high shear-sensitive thixotropic structure develops in boehmite sols upon introduction of Ce-salts. While as-synthesised boehmite suspensions are near-Newtonian and time-independent, Ce-modified boehmite sols exhibit increased viscosity, shear-thinning behaviour and thixotropy (Figs. 4 and 5). The thixotropic structure further increases when those sols are aged for 3 days.

The rate of structure formation in Ce-modified boehmite sols appears to be strongly dependant on the type of counterion used. The rheological data recorded in $Ce(NO_3)_3$, $CeCl_3$, $Ce(CH_3COO)_3$, and $Ce_2(SO_4)_3$ systems indicate that the shear-stress *vs.* shear-rate profiles are similar with the first three anions and differ with SO_4^{2-}. The particle network that forms at t_0 with $Ce(NO_3)_3$ and $CeCl_3$ is relatively weak (Fig. 5a). Ageing the sols for 3 days, involves a repulsive to adhesive transition in the particle–particle interactions. As a result of these adhesive interactions, an hysteresis loop develops in the shear-stress *vs.* shear-rate curves (Fig. 5b) the area of which reflects the degree of thixotropy of the sol. The evolution of the thixotropic structure was fast with $Ce(NO_3)_3$ and still much faster with $CeCl_3$. In contrast, $Ce(CH_3COO)_3$ presented a high thixotropic structure at t_0, suddenly after introduction of this salt, but the degree of thixotropy of the sol did not increase significantly with ageing.

It is generally accepted that, in the presence of inert electrolyte, particles bond together when the range of double layer repulsive interactions is sufficiently reduced to permit particles to approach one another to the point where the van der Waals attractive forces dominate [17]. The effect of the anion size from neutral salts has been investigated on aqueous suspensions of boehmite [17] and goethite (α-FeOOH) by potentiometric titrations [49]. It was found that gels form predominantly with monovalent anions when a critical ionic strength is reached, the value of which increases with increasing the size of the anion. In both studies, the data were explained using the idea that smaller anions are more efficient at approaching the surface of the particles than larger ones. As a result, the surface charge is screened and the diffuse portion of the double layer is compressed leading to a decrease of the interparticle repulsion.

In our systems, CH_3COO^- has the smallest ionic radius (R_i = 0.217 nm, Table 4) and its negative charge is concentrated on the two oxygen atoms. In aqueous solution, this anion is very strongly hydrogen bonded, so contributing to the negative enthalpy of hydration (−425 kJ mol^{-1}). This generates a thick hydration shell of ordered water molecules.

In agreement with the results of Gieselmann and Anderson [17], our data indicate that the slightly smaller CH_3COO^- anion is more effective at shielding the surface charge that develops on boehmite particles than the larger NO_3^- (R_i = 0.223 nm) and Cl^- (R_i = 0.224 nm) anions. This results in a strong decrease of the interparticle repulsion with $Ce(CH_3COO)_3$ and in the development of adhesive interactions leading to aggregation of particles in a highly thixotropic network.

However, the evolution of the thixotropic structure can not be explained only by the dimension of the counterions. Thus, we note that, although the hydrated ionic radii of nitrate and chloride ions are very close, a huge difference is observed in the evolution of the thixotropic structure of these sols (Fig. 6). This evolution is much stronger with $CeCl_3$ compared to $Ce(NO_3)_3$. Such behaviour has been observed also by other authors and may be explained by non-DLVO interactions, *i.e.* structured forces generated by the adsorbed layer of hydrated Cl^- ions (also called solvation forces) [52]. The thickness of these adsorbed layers follows the same order as the hydration enthalpy of the two ions, Cl^- (−365 kJ mol^{-1}) > NO_3^- (−312 kJ mol^{-1}) and the degree of coagulation of particles also follows this order.

The apparent viscosity measured at 1000 s^{-1} with $Ce(CH_3COO)_3$ was reduced after 3 days from 23.29 to 19.72 mPa s. This behaviour is similar to what has been observed with gibbsite suspensions. Gibbsite nanoparticle agglomeration has been shown to

Table 4
Values of ionic radius and hydration enthalpy at 25 °C of the studied counterions [50,51].

Counterion	Hydrated radius R_h (nm)	Hydration enthalpy (kJ mol^{-1})
NO_3^-	0.223	−312
Cl^-	0.224	−365
CH_3COO^-	0.217	−425
SO_4^{2-}	0.273	−1035

occur in two steps: firstly *via* reversible aggregation due to physical forces, followed by irreversible chemical cementation [5]. In the $Ce(CH_3COO)_3$ system, such behaviour may be explained by the fact that if the chemical agglomeration of the aggregates becomes significant, the total number of reversible particle–particle interactions may be reduced, leading to a decrease of the sol viscosity.

In the case of $Ce_2(SO_4)_3$, the situation is different. The shear-stress *vs.* shear-rate curve of this system presents a shear-thinning behaviour but thixotropy was evidenced neither at t_0 nor at t_{3d}. Thus, when boehmite sols were mixed with $Ce_2(SO_4)_3$, the sol spontaneously separated into a colloid-rich and a colloid-poor phase. This observation indicates that $Ce_2(SO_4)_3$ interacts in an unusual manner with boehmite nanoparticles. Indeed, sulphates have been shown to bond strongly to particles of goethite [53–55] and to favour the growth of boehmite along [100] direction [24]. The precipitation of boehmite in the presence of different anions (Cl^-, NO_3^- and SO_4^{2-}) has also been investigated [23]. From this study it was inferred that the hydrolysis of $Al_2(SO_4)_3$ starts at lower temperatures (compared to $AlCl_3$ and $Al(NO_3)_3$) due to the formation of hydroxy-sulphate species as a result of the higher complexing ability of SO_4^{2-} with aluminium compared to Cl^- and NO_3^-.

In order to corroborate our rheological results, we have undertaken vibrational spectroscopic experiments to highlight interactions between Ce-salts and the surface of boehmite nanoparticles. The positive surface charge of the boehmite implies its stabilisation by nitrate anions which could be free or coordinated to cerium and the IR spectroscopy ascertains identification of these two species.

Adsorption of nitrate anions on nanoparticle surface is demonstrated by FTIR and DRIFT spectroscopies (Fig. 3 and 7A, a). These anions come from peptization during which Al-OH is protonated in $Al\text{-}OH_2^+$. Protonation is followed by the adsorption of free NO_3^- ions on the nanoparticle surface by H-bond.

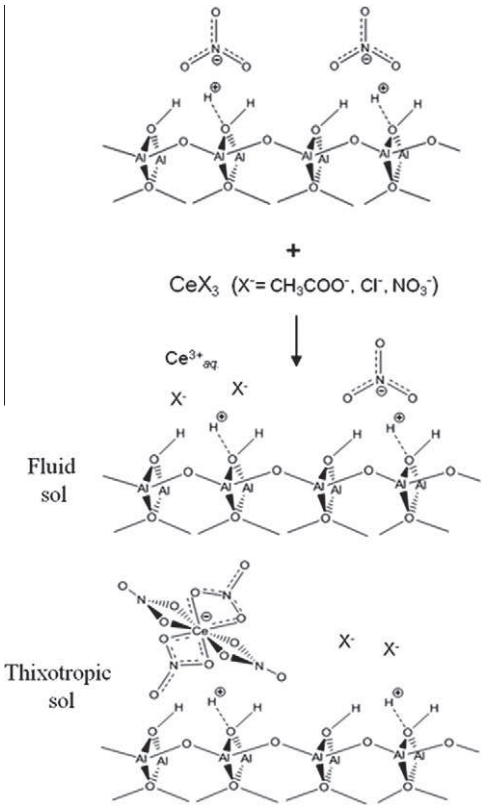

Fig. 8. Schematic illustration for nitric acid peptised boehmite before and after introduction of cerium salt in solution.

On Ce-modified boehmite (Fig. 7A, b–e), coordination between free NO_3^- anions and Ce^{3+} cations was evidenced by the splitting of the band at 1380 cm^{-1} in two bands at 1460 and 1345 cm^{-1}. Indeed, these two bands appear at the same positions as those of $Ce(NO_3)_3$ as solid (Fig. 7B, b).

Based on these observations, the interaction of $Ce(NO_3)_3$, $CeCl_3$ and $Ce(CH_3COO)_3$ with boehmite surface may occur as illustrated in Fig. 8. When these salts are introduced separately in the peptized boehmite sol, the coordination between Ce^{3+} cations and free NO_3^- surface anions leads to formation of $[Ce(NO_3)_4(H_2O)_x]^-$ complex ions which adsorb on the nanoparticle surface *via* H-bond. Such adsorption contributes to the modification of particle–particle interactions (from repulsion to attraction) and by consequence a thixotropic structure develops.

According to the results mentioned above, we can assume that the adsorption of Ce-salts at the boehmite–water interface strongly affects the rheological behaviour of the sols. More importantly, the nature of Ce-salts as well as the ageing time may be chosen appropriately to tune the sol viscosity.

5. Conclusion

Stable suspensions of boehmite crystallites were synthesised by hydrolysis and condensation of aluminium tri-*sec*-butoxide in water followed by peptisation with nitric acid. DRIFT data collected on boehmite sols showed one band at 1380 cm^{-1} associated to the adsorption of NO_3^- anions at the $AlOH_2^+$ sites of boehmite.

The addition of Ce-salts involved changes on the rheological behaviour of the sols. While Ce-free boehmite suspensions were near-Newtonian and time-independent, the addition of Ce-salts involved a high shear-thinning behaviour. Depending on the nature of Ce-salt used, the rheological behaviour of the sol was modified in a different way. The thixotropic structure that formed at t_0 was moderate in the sols prepared with $Ce(NO_3)_3$ and $CeCl_3$ whereas it was strongly enhanced in the sols prepared with $Ce(CH_3COO)_3$. After ageing the sols for 3 days, a higher evolution of the thixotropic structure was observed with $CeCl_3$ compared to $Ce(NO_3)_3$, whereas a saturation value was reached with $Ce(CH_3COO)_3$. By contrast, $Ce_2(SO_4)_3$ presented a sudden phase-separation due to the complexation of the anion with dissolved aluminium species.

DRIFT spectra collected from Ce-modified boehmite samples showed splitting of the band at 1380 cm^{-1} into two bands at 1460 and 1345 cm^{-1} which are associated to the coordination of free NO_3^- anions at the boehmite surface with Ce^{3+} ions followed by the formation of $[Ce(NO_3)_4(H_2O)_x]^-$ complex ions. Such Ce-complexes that adsorb at boehmite/water interface play a decisive role on the interparticle interactions and are probably at the origin of the thixotropic structure formation. Combining rheological data with data computed from IR spectroscopies may be a new approach to interfer information about the rheological behaviour of colloidal dispersions linked to complex formation at the particle/water interface.

Acknowledgments

This work was financially supported by DGCIS and the Regional Councils of Midi-Pyrénées and Aquitaine. The authors thank all industrial partners: Liebherr Aerospace, Ratier-Figeac, Eurocopter, Turbomeca, Messier Dowty, Messier Bugatti, Mecaprotec Industries, as well as IPREM, UPPA, Pau, FR.

References

[1] (a) I.J. Langmuir, Chem. Phys. 6 (1938) 873;
(b) J. Bugosh, J. Phys. Chem. 65 (1961) 1789.

[2] (a) A. Delville, J. Phys. Chem. B 103 (1999) 8296;
(b) M. Dijkstra, J.-P. Hansen, P.A. Madden, Phys. Rev. Lett. 75 (1995) 2236;
(c) M. Dijkstra, J.-P. Hansen, P.A. Madden, Phys. Rev. E 55 (1997) 3044;
(d) F. Pignon, A. Magnin, J.M. Piau, J. Rheol. 42 (1998) 1349.
[3] (a) J. Addai-Mensah, J. Dawe, R.A. Hayes, C.A. Prestidge, J. Ralston, J. Colloid Interface Sci. 203 (1998) 115;
(b) J. Addai-Mensah, A. Gerson, I. Ametov, C.A. Prestidge, J. Ralston, Light Metals 1 (1998) 159.
[4] (a) J. Labanda, J. Llorens, J. Colloid Interface Sci. 289 (2005) 86;
(b) J. Labanda, J. Llorens, Rheol. Acta 45 (2006) 305;
(c) J. Labanda, J. Sabaté, J. Llorens, Colloids Surf. A: Physicochem. Eng. Aspects 301 (2007) 8.
[5] (a) C.A. Prestidge, I. Ametov, J. Addai-Mensah, Colloids Surf. A: Physicochem. Eng. Aspects 157 (1999) 137;
(b) C.A. Prestidge, I. Ametov, J. Crystal Growth 209 (2000) 924;
(c) J. Li, C.A. Prestidge, J. Addai-Mensah, J. Colloid Interface Sci. 224 (2000) 317.
[6] P. Ghosh, Adhesives and Coatings Technology, Tata McGraw-Hill, New Delhi, 2008.
[7] D.L. Gamble, Industrial and Engineering Chemistry (1936) 1204.
[8] P.A. Buining, A.P. Philipse, H.N.W. Lekkerkerker, Langmuir 10 (1994) 2106.
[9] D.H. Han, O.O. Park, Y.G. Kim, Appl. Catal. B: Gen. 86 (1992) 71.
[10] C. Kropf, T. Foerster, M. Heller, M. Claas, B. Banawski, Verfahren zur Herstellung wässriger Gele und deren Verwendung zur Körperdeodorienung DE 19857235, A1, 2000.
[11] S. Ishida, N. Takeuchi, K. Fujiyoshi, Y. Michiie, T. Susuki, K. Kido, H. Kigata, H. Mitsunaka, Jpn. Pat. 20 041 (2004) 216.
[12] R. Tettenhorst, D.A. Hofmann, Clays Clay Miner. 28 (1980) 373.
[13] J. Peric, R. Krstulovic, M. Vucak, J. Therm. Anal. 46 (1996) 1339.
[14] J.F. Hochepied, P. Nortier, Powder Technol. 128 (2002) 268.
[15] H. Ginsberg, W. Huttig, H. Stiehl, Z. Anorg. Allg. Chem. 309 (1961) 233.
[16] (a) B.E. Yoldas, J. Mater. Sci. 10 (1975) 1856;
(b) B.E. Yoldas, Am. Ceram. Soc. Bull. 54 (1975) 286;
(c) B.E. Yoldas, Am. Ceram. Soc. Bull. 54 (1975) 289;
(d) B.E. Yoldas, US Patent 941 (1976) 719.
[17] M.J. Gieselmann, M.A. Anderson, J. Am. Ceram. Soc. 72 (1989) 980.
[18] P. Alphonse, R. Bleta, R. Soules, J. Colloid Interface Sci. 337 (2009) 81.
[19] R. Bleta, P. Alphonse, L. Lorenzato, J. Phys. Chem. C 114 (2010) 2039.
[20] M. Dj. Petkovic, S.K. Milonjic, V.T. Dondur, Bull. Chem. Soc. Jpn. 68 (1995) 2133.
[21] R. Petrovic, S. Milonjic, V. Jokanovic, Lj. Kostic-Gvozdenovic, I. Petrovic-Prelevic, Dj. Janackovic, Powder Technol. 133 (2003) 185.
[22] J.D.F. Ramsay, S.R. Daish, C.J. Wright, Materials Physics Division, AERE, Harwell (1977) 65.
[23] D. Mishra, S. Anand, R.K. Panda, R.P. Das, Mater. Lett. 53 (2002) 133.
[24] T. He, L. Xiang, S. Zhu, Langmuir 24 (2008) 8284.
[25] G. Johansson, Acta Chem. Stand. 14 (1960) 771.
[26] P. Alphonse, M. Courty, J. Colloid Interface Sci. 290 (2005) 208.
[27] Z.J. Li, M. Flytzani-Stephanopoulos, J. Catal. 182 (1999) 313.
[28] J.H. Osborne, K.Y. Blohowiak, S.R. Taylor, C. Hunter, G. Bierwagen, B. Carlson, D. Bernard, M.S. Donley, Prog. Org. Coat. 41 (2001) 217.
[29] B.F. Rivera, B.Y. Johnson, M.J. O'Keefe, W.G. Fahrenholtz, Surf. Coat. Technol. 176 (2004) 349.
[30] G. Skillas, Z. Qian, U. Baltensperger, U. Matter, H. Burtscher, Combust. Sci. Technol. 154 (2000) 259.
[31] W. Zhang, T.J. Pinnavaia, Chem. Commun. (1998) 1185.
[32] M.L. Zheludkevich, R. Serra, M.F. Montemor, K.A. Yasakau, I.M. Miranda Salvado, M.G.S. Ferreira, Electrochim. Acta 51 (2005) 208.
[33] A.E. Hughes, J.D. Gorman, P.R. Miller, B.A. Sexton, P.J.K. Paterson, R.J. Taylor, Surf. Interface Anal. 36 (2004) 290.
[34] W O Milligan, J. Phys. Chem. 60 (1956) 273.
[35] J.J. Fripiat, H. Bosmans, P.G. Rouxhet, J. Phys. Chem. 71 (1967) 1097.
[36] Ph. Colomban, J. Mater. Sci. 24 (1989) 3002.
[37] K. Nakamoto, Infrared and Raman Spectra of Inorganic and Co-ordination Compounds, John Wiley & Sons, Hoboken, New Jersey, 2009.
[38] F. Pignon, J.M. Piau, A. Magnin, Phys. Rev. Lett. 76 (1996) 4857.
[39] H.A. Barnes, J. Non-Newtonian Fluid Mech. 7 (1997) 1.
[40] B.V. Deryagin, L. Landau, Acta Physicochim. URSS 14 (1941) 633.
[41] A. Halfon, S. Kaliaguine, Can. J. Chem. Eng. 54 (1976) 168.
[42] H. Green, R.N. Weltmann, Ind. Eng. Chem. Anal. Ed. 18 (1946) 167.
[43] D. Perret, J. Locat, P. Martignoni, Eng. Geol. 43 (1996) 31.
[44] W.H. Herschel, R. Bulkley, Kolloid-Z. 34 (1926) 291.
[45] E.C. Bingham, Fluidity and Plasticity, McGraw-Hill, New York, 1922 (Chapter 8).
[46] D. Fauchadour, F. Kolenda, L. Rouleau, L. Barre, L. Normand, Stud. Surf. Sci. Catal. 143 (2002) 453.
[47] C.R. Evanko, R.F. Delisio, D.A. Dzombak, J.W. Novak Jr., Colloids Surf. A Physicochem. Eng. Aspects 125 (1997) 95.
[48] S.A. Cotton, C.R. Chimie 8 (2005) 129.
[49] D.E. Yates, T.W. Healy, J. Colloid Interface Sci. 52 (1975) 222.
[50] Y. Marcus, J. Chem. Soc. Faraday Trans. 87 (1991) 2995.
[51] Y. Marcus, Ion Properties, Marcel Dekker, New York, 1997.
[52] M. Hosokawa, K. Nogi, M. Naito, T. Yokoyama, Nanoparticle Technology Handbook, Elsevier Science, Linacre House, Jordan Hill, Oxford OX2 8DP, UK, 2007.
[53] S.J. Hug, J. Colloid Interface Sci. 188 (1997) 415.
[54] H. Wijnja, C.P. Schulthess, J. Colloid Interface Sci. 229 (2000) 286.
[55] D. Peak, R.G. Ford, D.L. Sparks, J. Colloid Interface Sci. 218 (1999) 289.